Modelling and verification of sesame seed particles using the discrete element method

Noureldin Sharaby,[1,2] Artyom Doroshenko,[1] Andrey Butovchenko[1]

[1]Don State Technical University, Rostov-on-Don, Russian Federation; [2]Agricultural Engineering Department, Faculty of Agriculture, Kafrelsheikh University, Egypt

Abstract

The size of sesame seed particles has been measured and analysed to build a sesame seed particle model using the discrete element method (DEM). Despite the strength of simulations using the DEM method, one of the challenges that still require to be overcome is approximating the form of the actual particles, especially for irregular shapes, to obtain more realistic simulations. Thus, the sesame seed particle was simplified to be quite close to the actual seed forms by drawing an irregular 3D sesame particle model using Fusion 360 software with the average dimensions of five hundred randomly selected sesame seeds. Consequently, a modelling approach for sesame seed particles based on a multi-sphere (MS) method was suggested. In this paper, the simulated results of the sesame particle model were close to those obtained experimentally, with 28 filling spheres. The results for both piling tests and oscillating seed meter calibration have shown that the 28-sphere model is appropriate for modelling the sesame seed particle. Thus, the validity and feasibility of the modelling approach for sesame seed particles we proposed have been verified. Finally, the simulation analysis provided a good prediction for the outflow process of sesame seeds from the oscillating seed meter. The optimum values for the main parameters of the oscillating seed metering device for sowing sesame seeds are 9 mm for seed exit hole clearance, 20° for oscillation angle, and 0.022 sec for opening time, providing a sesame seed rate of 2.7 kg/ha. As a result, it provides a reference for the design and optimisation of oscillating seed meter for sowing sesame seeds.

Correspondence: Noureldin Sharaby, Agricultural Engineering Department, Faculty of Agriculture, Kafrelsheikh University, Kafrelsheikh 33516, Egypt.
Tel.: +201030257023.
E-mail: Noureldin_Sharaby@agr.kfs.edu.eg ; sharaby_nor@yahoo.com

Key words: Discrete element method; multi-spheres; oscillating seed meter; sesame seed; simulation analysis.

Acknowledgements and funding: this work was supported by Don State Technical University, 344000 Rostov-on-Don, Russian Federation.

Received for publication: 29 September 2021.
Accepted for publication: 3 March 2022.

Journal of Agricultural Engineering 2022; LIII:1286
doi:10.4081/jae.2022.1286

Introduction

Sesame seed (*Sesamum indicum* L.) is considered one of the most important oil crops in the world, which has a high level of oil content (50-60%) and protein (18-25%) (Borchani *et al*., 2010; Noorka *et al*., 2011). Sesame seed has a high nutritional value, rich protein, phosphorus, and calcium content. In recent years, there has been a globally increasing demand for its seed and sesame oil. Thus, it has led many countries to produce and export sesame, as it is one of the primary sources of foreign currency for many countries, especially in Africa and Asia (Sharaby and Butovchenko, 2019).

During the different processes of handling sesame seeds in agricultural operations such as sowing, harvesting, threshing, separation, processing, and packing, there is friction between the sesame particles; moreover between sesame particles and the related mechanical parts during the various processes. Therefore, it is crucial to create a precise model for gathering sesame seeds to analyse these contacts to optimise the relevant mechanical parts using the discrete element method (DEM), which was recognised as a numerical tool for simulating granular material (Cundall and Strack, 1979). Granular materials play an essential role in several agricultural and industrial applications. Since ancient times, they have been present in the human economy in such forms as cereal grains and construction materials.

In recent years, the discrete element method has been widely used as a leading tool for describing various issues in granular processes, including many industrial applications, and agricultural industries, due to the rapid development of computing power and advanced contact algorithm. The importance of using the discrete element method approach is becoming more popular for studying and analysing the dynamic behaviour of the granular materials and their kinematic pattern of motion at the particle interaction level (Härtl and Ooi, 2008; Ramírez *et al*., 2010). DEM simulations have been extensively applied to various problems regarding agricultural granular materials. It has been successfully applied and has proven effective in studying various technical and agricultural simulation processes (Guo *et al*., 2012; Boac *et al*., 2014; Horabik and Molenda, 2016; Leblicq *et al*., 2016).

Many agricultural granular materials such as grains and seeds have non-spherical shapes. The accurate representation of the

agricultural granular particle shape is the key to DEM simulations and obtaining more accurate results. Therefore, many researchers have simplified the different shapes of several agricultural seeds to an ellipsoid (Lin and Ng, 1995; Ouadfel and Rothenburg, 1999). However, the contact detection algorithms for ellipsoids are more complex, which leads to a long computational time (Kruggel-Emden *et al*., 2008).

Recently, many investigators employed the multi-sphere (MS) approach to describe complex material geometries, in which a certain number of spheres were *glued* together. Most authors use multi-spherical particles to build agricultural grains particle models for different types of seeds for modelling elongated particles of irregular shape based on the multi-sphere method and building analysis models of agricultural grains (Markauskas *et al*., 2015; Radvilaitė *et al*., 2016; Wang *et al*., 2017). Therefore, different sphere numbers are used to represent the shape of the grains. The sphere numbers depend on the irregularity of the grain shapes to give simulation results consistent with experimental results. For example, Xu *et al.* (2018) built a model of soybean seed with different sizes and distributions using 5, 9, and 15 spheres, while Chen *et al.* (2018) were built a particle for maize seed assembly model for different types of maize using different numbers of spheres for filling it from 1 to 25 sub-spheres. A good agreement of numerical and experimental results regarding the discharge time and repose angle of the pile was reached simultaneously when the final particle model examined by Markauskas and Kačianauskas (2011) was composed of 11 spheres to investigate rice grain flow by multi-sphere particle model with rolling resistance. Boac *et al.* (2010) tested a particle model for simulating soybeans in grain handling and enhancing the prediction of grain commingling in bucket elevator equipment. A particle model with a single sphere best-simulated soybean kernels in the bulk property tests compared to 2-sphere, 3-sphere, and 4-sphere models. To replicate an ellipsoidal wheat grain and save computational time, Weigler and Mellmann (2014) checked different arrangements and numbers of spheres in the particle flow simulations to find the optimal number of spheres, which was five. Thus, considering the accuracy in describing the shape of agricultural granular particles and computational effort, the appropriate geometrical shape of irregular particles should be carefully modelled. Models with different spheres generally have different characteristics. However, the number of spheres demands further research for agricultural grains with unequal sizes. To date, it is evident that studies using the multi-sphere model as a non-spherical particle shape method have shown various details and frictional behaviour of different material properties and specified numerical model parameters. Besides, the sizes of each sesame seed differ within the same variety. Therefore, a clear need exists for building a sesame seed particle model with a size distribution consistent with the actual one. We verified the accuracy of a particle model by comparing the simulated and experimental results. However, these methods reflect the influence of the particle assemblies instead of individual particles. Thus, current verification methods are insufficient.

This paper used sesame seeds to measure and analyse their shapes and sizes. The study evaluates and verifies various parameters for a single sesame seed particle and sesame seed assembly using the multi-sphere method by comparing the simulated and experimental results. This study aims to find the optimal values for the basic parameters of the oscillating seed metering device for sowing sesame seeds. These data are necessary for designing working bodies and affect the flow of technological processes using the discrete element method. The simulation analysis for the working process of the oscillating seed metering device for sowing sesame seeds has not been previously performed. This work will provide a reference for related research.

Materials and methods

Measurement and analysis of the size of sesame seeds

In this paper, we use sesame seeds (*Solnechniy* variety) as the research object. The sesame seed particle was modelled with identified sizes and shapes similar to actual seed forms, making the particle modelling easier and giving results closer to the experimental results. Sesame seeds are difficult to represent as an ellipsoid. Thus, an irregular 3D sesame seed particle was performed using Fusion 360 software with a similar size to the actual one, namely, thickness (T), width (W), and length (L). The sesame particle was used in the modelling process to determine the number of spheres required to build the sesame particle model. Therefore, the problem is determining the size of each particle within the assembly for modelling a sesame seed. This work randomly selected five hundred intact seeds from sesame seeds. The sesame dimensions were measured with a digital Vernier calliper with an accuracy of 0.01 mm. The results are listed in Table 1, and it showed that sesame sizes followed a normal distribution. The distributions of the sizes using sesame seeds are shown in Figure 1.

The actual sesame three dimensions (length, width, and thickness) were used to create sesame seed particles; thus, the size and distribution of the generated seeds particle assembly were very similar to those of the actual sesame seeds.

Modelling method of sesame seed particle assemblies

DEM simulation was performed with a commercially available DEM software (EDEM_3.0 analysis), which treated particles as soft sphere models. In several recent studies, irregular particles are often modelled in EDEM simulations by applying a multi-sphere approach, which uses several spheres assembly as a simulation

Table 1. Some physical properties of a sesame seed (*Solnechniy*).

Physical properties	Mean	Standard deviation
*Length (*L), mm	3.254	0.202
Width (*W*), mm	1.867	0.145
Thickness (*T*), mm	0.925	0.095
Mass of 1000 seeds, g	2.70	-
Mean volume of one particle, mm^3	2.6491	-
True density, $kg.m^{-3}$	603	-

particle, which is shapely with an irregular particle outer contour, such as maize (Ren *et al*., 2012) and rice (Lei *et al*., 2016). Therefore, to describe the sesame seed, which has an irregular shape with the largest thickness and width in the middle and gradually decreases as moving toward the two ends of the sesame seed. The sesame seed has two sides; one has a pointed, less thick and wide shape, and the other end has a curvature shape.

The modelling approach for a single sesame seed particle was as follows: the sesame particle was simplified by drawing a 3D sesame seed particle model with an irregular form that is entirely similar to the actual sesame one. The single sesame particle size was identical to the mean values of an actual sesame particle assembly; the single sesame particle was modelled by the filling-spheres method (Figure 2A). The particle model of a single sesame seed, as mentioned above, is considered a template.

There is no specific number of spheres representing the sesame seed particle in EDEM simulations. In addition, no previous studies for validating and modelling the sesame seeds have been performed to date except for the study carried out by Sharaby *et al*. (2020), as they built a sesame seed model using a 12-sphere model for filling sesame particles; thus, the discrete element modelling of sesame seed assembly still needs to be further study. Therefore, in this study, the different sphere numbers (9, 11,15, 19, and 28 sub-spheres) were used to fill and build a sesame seed particles model to perform a simulation using DEM. Spheres with different diameters have been selected to represent the thickness (T) of the sesame seed that does not have a uniform thickness for the same seed because of the difference in the thickness of the sesame seed in the direction of the other two dimensions of the seed (L and W). Sesame seed particle lie is related to the X, Y, and Z axes of the space coordinate system. The spheres overlap at different distances, as attributed to the X and Y axes on the XOY plane, representing both width and length, respectively, to form the sesame seed particle (Figure 2).

Establishment of sesame seed model (9, 11, 15, 19, and 28-sphere)

The filling method of the nine-sphere model (9s) was as follows: on the XOY plane, the centre of the sesame seed particle was firstly filled with a four sphere with a diameter equal to sesame thickness (0.9 mm), which are symmetrically on both sides of the X and Y axes, so that they are away from the length axial (±Y axial), with a distance of (±0.4 mm) and from the width axial (±X axial), with a distance of (±0.3 mm) as shown in Figure 2B. Similarly, four additional spheres (0.7 mm) were used to fill the sesame particle, on either side of the longitudinal axes of the sesame seed particle (±Y axial), with (±0.3 mm), and from the width axial (±X axial), with a distance of (±0.9 mm). Finally, one sphere with a diameter of 0.5 mm was filled in the pointed part of the sesame particle, as its centre is on the length axial (–y axial) and away from the width axial (–x axial), with (–1.4 mm). As a result, the 9s model is established. Thus, the nine-sphere model is the simplest model to fill a sesame seed particle, based on the multi-sphere method during EDEM simulations.

Because of large voids between the spheres along Y-axes for the nine-sphere sesame model, the filling process is continued for building the 11-sphere model (11s), as shown in Figure 2C.

Evidently, from both previous models (9s and 11s). However, they did not fully cover the sesame particle width without affecting the sesame seed thickness since there are some voids between

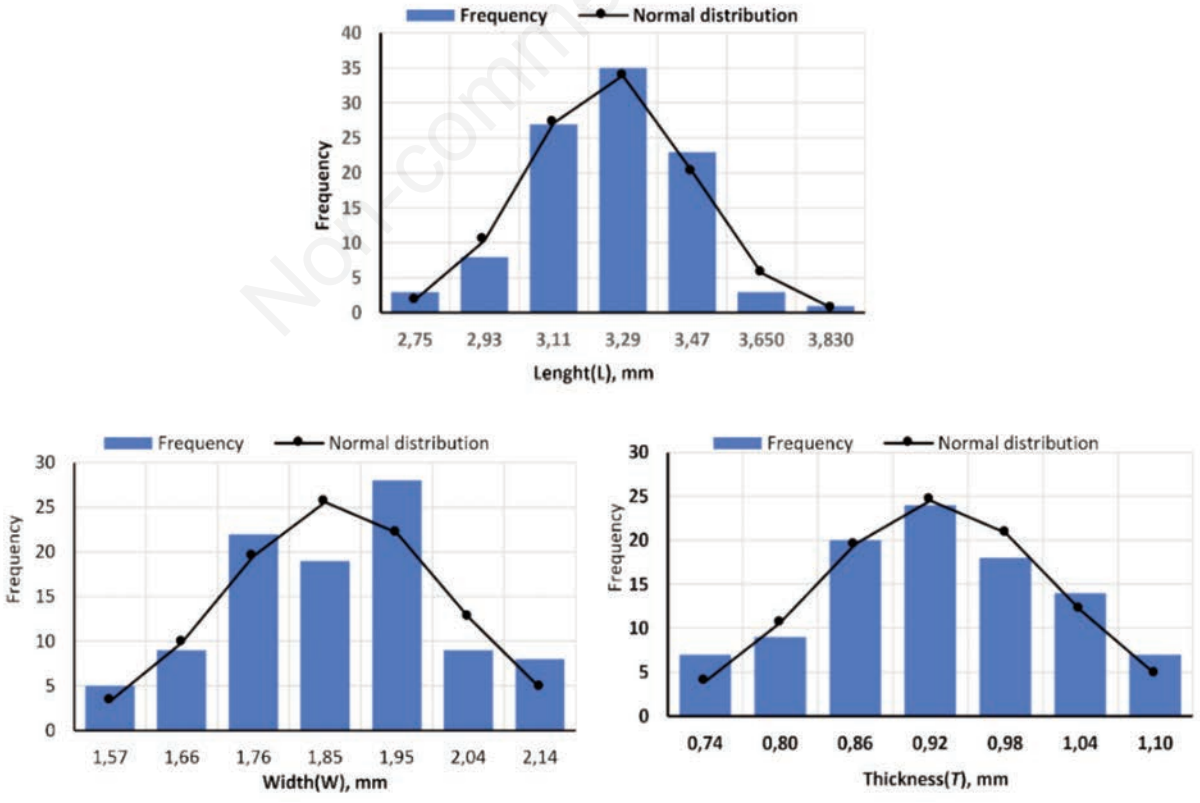

Figure 1. Distribution of sizes of sesame seeds: thickness(T), width(W), and length(L).

spheres and a large waviness on the outside of the sesame particle. Therefore, with the same approach, the number of spheres has been increased to 15-sphere to represent the seed particle more realistically. As a result, the 15-sphere model (15s) gives the actual dimensions of a sesame seed.

Although the 15-sphere model covered the actual sesame particle width, there were small voids between some spheres during the building of the model. Therefore, to reduce the waviness and overcome the gaps between the spheres in the previous models (15s), the 19-sphere model (19s) is established (Figure 2E) to approximate the actual sesame particle shape, preserving the real dimensions of the sesame seed size (length, width, and thickness).

How many spheres represent the sesame particle shape using DEM simulations to answer this question. Therefore, the particle was formed with different sphere numbers (9, 11, and 15-sphere). After that, the approach usually consists of increasing the number of spheres to reduce the waviness effect. Therefore, the sesame particle was filled with a 19-sphere model without knowing the exact number of spheres. However, the more spheres, the less waviness effect and the model becomes more realistic. With the same approach, the filling method of the 28-sphere model (28s) was oriented to achieve the most realistic smoothening, as shown in Figure 2F.

In this work, based on the filling methods mentioned above, five particle models (9, 11, 15, 19, and 28-sphere models) were built for a single sesame seed particle, as illustrated in Figure 3. The multi-sphere method makes the assembly model of sesame particles closer to the real one.

Experiment analysis and validation

In this part, the validation of the modelling method for the sesame particle assembly is proposed and performed. The piling tests were used to verify and compare simulation results for particle models (9, 11, 15, 19, and 28-sphere) with the experimental results of the static angle of repose.

In this work, the no-slip Hertz-Mindlin contact model was employed to simulate the sesame seed particles in an oscillating seed metering device, commonly used for simulating seed metering devices within EDEM simulations (Khatchatourian *et al*., 2014; Hongxin *et al*., 2015; Li *et al*., 2015; Jia *et al*., 2018). Hertz-Mindlin contact model is the default model used in software EDEM because of its accurate and efficient force calculation; and less computational effort (Cundall and Strack, 1979) developed the principle of the discrete element method (DEM simulation). Newton's second law and the Eulerian equation are usually used to describe the translational and rotational movements of a multi-sphere particle assembly and use a contact law to resolve contact forces.

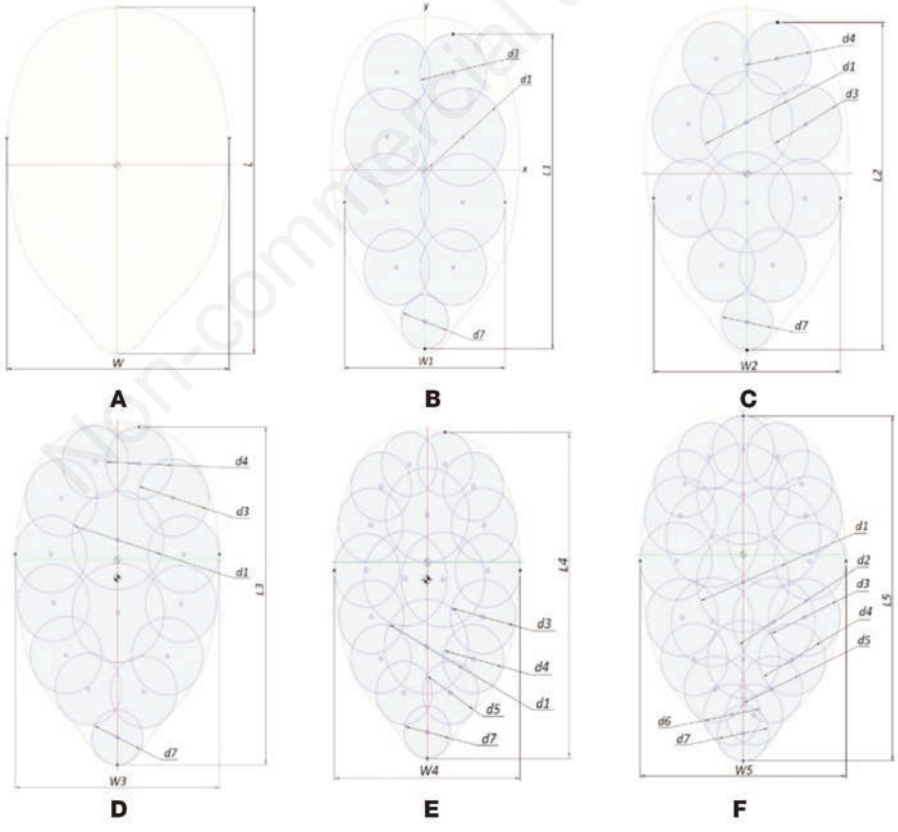

L=3.11	L_1=2.9	L_2=2.94	L_3=3.059	L_4=3.09	L_5=3.11	Dimensions
W=2.005	W_1=1.7	W_2=1.826	W_3=2	W_4=2	W_5=2.002	in mm
d_1=0.9	d_2=0.8	d_3=0.7	d_4=0.65	d_5=0.6	d_6=0.55	d_7=0.5

Figure 2. Filling methods for different multi-sphere models: A) sesame seed particle; B) 9-sphere model; C) 11-sphere model; D) 15-sphere model; E) 19-sphere model; and F) 28-sphere model.

Experiment analysis

Piling tests

The piling tests were carried out on a squarer container of glass plates (Figure 4) with dimensions of 200, 200, and 34 mm for length, height, and width, respectively. The glass plate thickness was 4 mm. The container was divided into two equal parts. Two movable panels moved between these parts on two other fixed plates with a distance of 0.6 mm. The piling tests were performed as follows: i) the upper part of the container was filled with sesame seeds (approx. 107 g) until it reached a pre-determined specific height; then, a scraper flattened the upper surface of the sesame seed; ii) the movable panels were pulled out, and the sesame seeds began to fall and pile until stabilised. Based on the pilling test, two different types of angles of repose can be obtained, namely, the internal (or drained) angle of repose (α) and the external (or poured) angle of repose (θ) (Johnston *et al*., 2009); iii) finally, the internal angle of repose was formed on both sides of the container's upper part (Zhou *et al.*, 1999); the external angle of repose was formed on both sides of the sesame pile after sesame seeds fell into the bottom of the square container. The entire process was monitored and recorded by a high-speed camera. The final value for the external angle of repose was determined as the average of the two static angles of repose. Similarly, the final internal angle of repose was determined as the average of the angles of the slope on two sides of the sesame pile in the container. The process case was repeated five times, and the mean value for the five experiments was used as the final results of the pilling test for each internal and external angle of repose.

Simulation study

Simulation processes were performed under conditions like those used in the experiments to test the validity of the proposed approach more quantitatively. For example, simulation times, the geometric dimensions of the square container, the volume of the sesame used, and the average mass of one sesame seed is equal to the mean volume of one particle for all sesame models.

Before performing a simulation analysis for sesame seeds using EDEM software, some relevant simulation parameters need to be determined: the interaction parameters between the particle and the material property parameters (Horabik and Molenda, 2016). The interaction parameters include the static friction coefficient, the restitution coefficient, and the rolling friction coefficient. While density, Poisson's ratio, shear modulus shape, and size distribution are part of material property parameters.

The piling process was simulated, as described above, for the sesame seeds. In this study, 9, 11, 15, 19, and 28-sphere models have been created to compare the effects of using different filling spheres for building the sesame particle models on the simulated results. The particle models (9s, 11s, 15s, 19s, and 28s) of sesame seeds were used in the simulations. The optimal number of filling spheres for building a sesame particle model is determined by comparing the simulated results with the corresponding experimental results for original sesame seeds. The simulation time of the 'piling test' for sesame seeds with EDEM_3.0 analysis software was 3.0 s, and the parameters used in the simulations are presented in Table 2.

The volume of sesame seeds used in the experimental process was the same volume during the simulation process for all sesame seed particle models. Also, the mass value of one sesame particle for all models in the simulation process was equal to the average mass of one original seed as an average of the five hundred sesame seeds used in the piling tests.

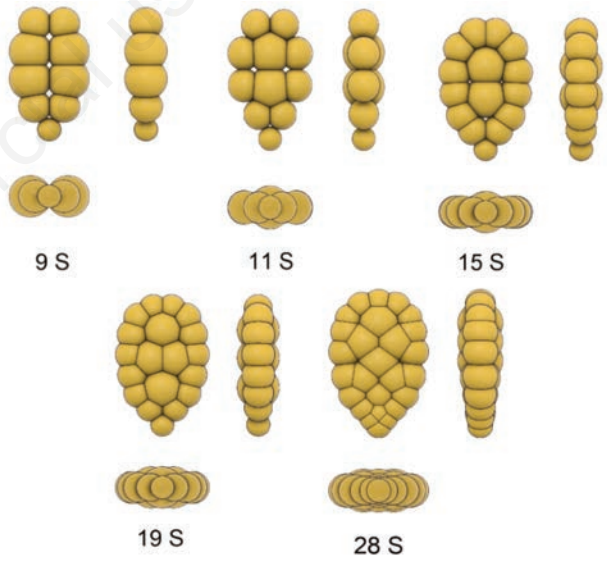

Figure 3. Sesame seed particle-based multi-sphere 5 models (9s, 11s,15s, 19s, and 28s).

Table 2. Input physical parameters used in the simulations.

Parameters	Symbol	Sesame seeds	Glass	Mild steel
Density (kg.m^{-3})	ρ	850	2500	7800
Poisson's ratio	υ	0.28	0.22	0.303
Shear modulus (Pa)	G	1·107	7·1010	7.93·1010
Restitution coefficient (with particle)	e	0.2	0.2	0.28
Static friction coefficient (with particle)	μ	0.35	0.39	0.52
Rolling friction coefficient (with particle)	μ_T	0.1	0.1	0.15

Verification of the oscillating seed metering device - Oscillating seed meter - Experiment analysis

Structure and working principle of oscillating seed metering device

This study used the oscillating seed metering system to analyse the oscillating meter operational performance for sowing sesame seeds. The structure of the oscillating metering device model consists of a seed hopper, metering device case, seed metering plate, stepper motor, two seed exit holes, and seed delivery tube, as shown in Figure 5. The experiments were carried out by filling the hopper with sesame seeds. The rectangular oscillating plate made of mild steel with dimensions of 57×22×1.5 mm for length, width, and thickness, respectively transmits the sesame seeds from the oscillating seed meter to the soil surface through seed exit holes under the influence of oscillating seed plate movement, which is driven by a stepper motor. The oscillating seed meter device is distinguished by its simple design and requires low power (12V) as it is controlled by an electric motor instead of a ground wheel and chain. It offers significant advantages over traditional mechanical and pneumatic seed metering technology. The oscillating seed meter simplifies maintenance by eliminating the drive chains, shafts, and sprockets-well, which are all still used in mechanical seed metering systems. The operation of the oscillating sowing unit also overcomes the sliding ground wheel and chain vibration, especially at high operating speeds, which affects the seed distribution uniformity. In addition, it does not include a vacuum system for sowing seeds as on a pneumatic metering device; as a result, it saves required power for the seeding process. In addition, it does not lead to seed disc clogging while seeding small-sized seeds such as sesame seeds. The particle of sesame seeds is used as the research object, so the outflow of the sesame seeds in the oscillating seed meter is recorded with a high-speed camera.

Oscillating seed metering control system

The oscillating seed metering control system is developed to optimise and control the sesame flow rate and improve seed spacing uniformity using an oscillating seed metering system. As shown in Figure 6, the main components of the oscillating seed metering device control system were the motor and its driver module, the input keyboard with LCD screen, the device programmer, the microcontroller, and the power source. The oscillating seed metering device works as follows: The input data representing operating parameters (seed exit hole clearance, opening time, and oscillation angle) are entered by typing them on the keyboard and appear simultaneously on the LCD screen. A microcontroller (ATmega 162AU) was selected to receive the input data after being processed through the device programmer (AVRISP mkII) to pro-

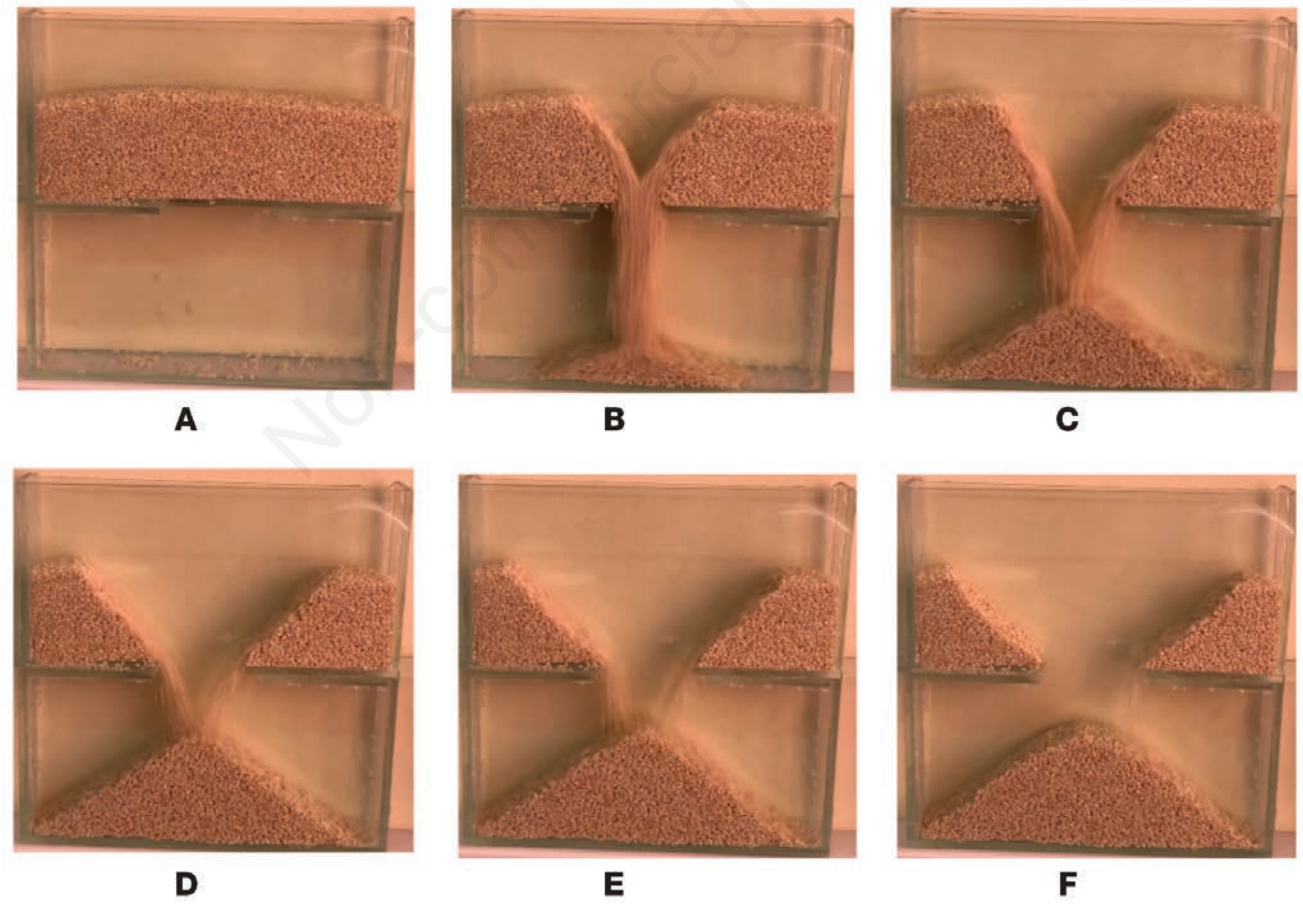

Figure 4. Photographs of the piling process of sesame seeds at different discharge times: A) t=0.00 s; B) t=0.50 s; C) t=1.00 s; D) t=1.50 s; E) t=2.00 s; and F) t=3.00 s.

vide appropriate pulses to the motor driver module. The output of the microcontroller was the pulses corresponding to these inputs. In this study, a stepper motor (23H2A0618) with a torque of 3 N.m. and a maximum current of 4.0 A was used based on the basic parameters described in detail below under the section 'Design parameters of the oscillating seed meter' for driving the oscillating seeding plate. A driver module has changed the rotation direction and speed of the stepper motor. A battery (12 V/60 A·h) supplied the electrical power, so the voltage of the stepper motor was estimated to be 12 V.

Initial experimental test

The laboratory experiments were conducted in the Agricultural Machinery Lab, Don State Technical University, Russian Federation, to collect data for model validations. The experiment had the exact dimensions of the oscillating metering device used in the model. The initial simulation using EDEM and the oscillating seed meter's laboratory experiments were performed with different opening time and oscillation angle values. In this study, based on the results from the initial simulation and laboratory experiments, values of the opening time, and oscillation angle, were determined at 25 ms and 20°, respectively, to study and analyse the effect of the seed exit hole clearance on the sesame seed outflow.

Design parameters of the oscillating seed meter

In this study, before running the EDEM model, simulation trials were designed to have the three most critical operating parameters of the oscillating seed metering system: seed exit hole clearance (cl), opening time (t), and oscillation angle (α), as shown in Figure 7, which might affect the sesame flow rate of oscillating

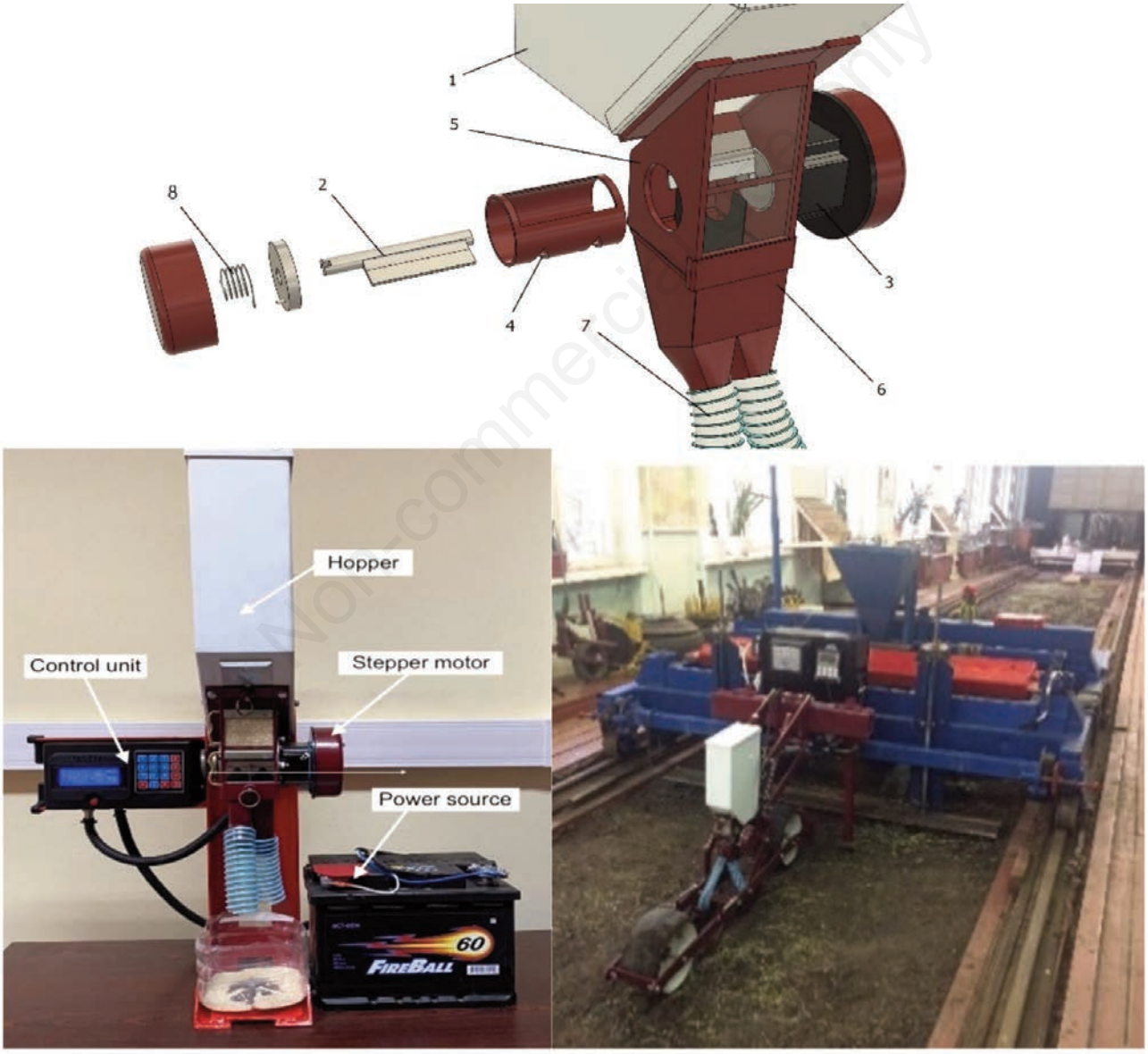

Figure 5. Structure, components, and tested oscillating seed metering device: 1. Seed hopper; 2. Oscillating seed plate; 3. Stepper motor; 4. Seed exit holes; 5. Metering device case; 6. Seed delivery tube; 7. Seed tube; 8. Coil spring.

seed metering device. The initial simulation using EDEM modelling and initial laboratory experiments of the oscillating seed meter was performed with different clearance, opening time, and oscillation angle values to study and analyse the sesame outflow from the oscillating seed metering device using the 28-sphere sesame particle model. The critical experiment parameters in the oscillating metering device were:

i) Seed exit hole clearance (cl)

During the oscillating seed metering device operation, sesame seed has low shear strength, and is lightweight and small-sized. Consequently, some sesame seeds were cut while falling from the seed exit hole into the seed delivery tube. Moreover, the flow rates of sesame from the oscillating seed metering device were irregular when the initial experiments did not consider the clearance value. Therefore, in this study, to overcome these problems, clearance values were determined from –10 to 30 mm to evaluate the effect of clearance on the sesame seeds' flow rate from the oscillating seed metering device, shown in Figure 8. The clearance required in mm represents the vertical distance between the upper edge of the seed exit hole and the upper edge of the oscillating seed plate at its maximum height at the top before moving down. According to the above experimental and simulation analysis, the main factors and levels table of tests are shown in Table 3.

ii) Opening time (t)

The opening time (in ms) is the time for the oscillating seed plate to move down from the top to a specific position based on the

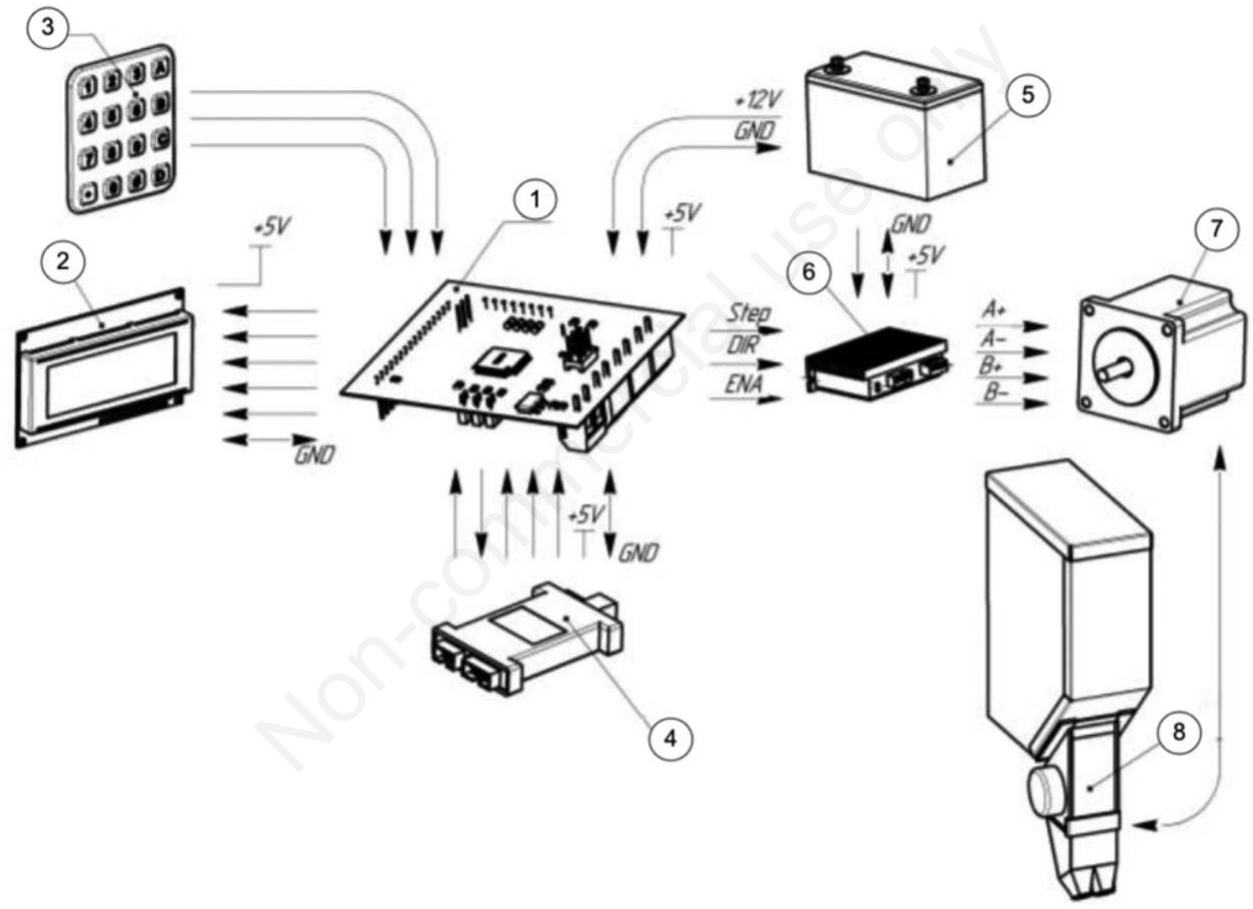

Figure 6. Schematic diagram of the oscillating seed metering control system: 1. Microcontroller; 2. LCD screen; 3. Input keyboard; 4. Device programmer; 5. Power source; 6. Stepper driver; 7. Stepper motor; 8. Oscillating seed meter.

Table 3. Factors and levels in experiments.

Factor name and unit of measurement	Factor levels			Variation interval
	Low (–1)	Middle (0)	High (+1)	
α - is the angle of motion for the oscillating seed plate (x_1), deg.	18	20	22	2
t - is the rotation time of the oscillating seed plate (x_{32}), sec.	0.02	0.025	0.03	0.005
cl - is the vertical distance between the upper edge of the seed exit hole and the upper edge of the oscillating seed plate (x_3), mm.	3	8	13	5

oscillation angle value (α) (Figure 7). Opening time affects the sesame outflow as it gives the seeds enough time or not to fall through the seed exit holes into the seed delivery tube. The opening time is controlled by regulating the oscillatory motion of the seed plate using an electric motor.

iii) Oscillation angle (α)

It is the angle of motion for the oscillating seed plate from the top to down during a specified opening time (t) (Figure 7), and it matches the angle of movement by the oscillating seed plate as it moves from down to top in the opposite direction by the coil spring. The oscillation angle value affects the sesame flow rate from the oscillating metering device, as the higher the oscillation angle value, the greater the sesame seed flow rate.

Results and discussion

Comparison between the experimental and simulated results for piling tests

During the simulation process, the sesame particle was filled with various spheres (9, 11, 15, 19, and 28-sphere) to select the optimal sesame model, giving the results closer to the actual sesame seed. During the initial experiments, the density of sesame particles was adjusted in the EDEM simulation (1200 kg.m^{-3}) to obtain the true density of sesame seed (603 kg.m^{-3}). Then, the simulation was performed to determine the densities of the different sesame particle models. The densities of all sesame particle models resulting from the simulation process were different according to the number of spheres used to build the sesame model, as shown in Table 4. For example, the obtained true density for the simulation 28-sphere sesame model was 602.798 kg/m^3, which was closest to the true density of actual sesame (603 kg/m^3) used in laboratory experiments compared with other models.

Figures 4 and 9 show photographs of experimental sesame seeds and snapshots of the sesame particle during the piling test simulation at different discharge times, respectively. The simulated sesame particle flow patterns are relatively consistent with those experimentally. When the simulation was completed, the angles of the slopes on both sides of the upper zone of the apparatus were measured. The averaged value of these two angles is considered the internal angle of repose resulting from the simulation process. Similarly, the slope angles of both sides were measured for the sesame pile located at the bottom zone of the device. The averaged value of these two angles is considered the external angle of repose.

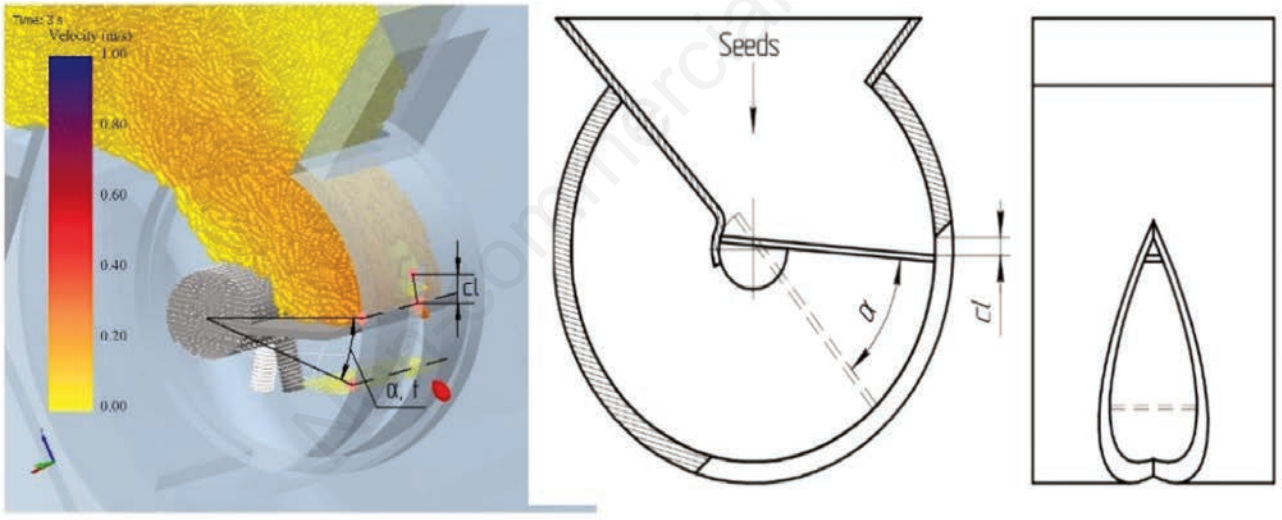

Figure 7. Snapshot of sesame flow rate simulation from the oscillating metering device under main operational parameters (seed exit hole clearance, opening time, and oscillation angle) using EDEM.

Table 4. The numbers of multi-spheres and particles used in a simulation process in the pilling test and obtained sesame particles' true density for a different number of filling spheres.

Models	No. of sesame seed particles	No. of multi-spheres	Volume of one particle, mm^3	Sesame particle true density, kg.m^{-3}
9 s	19,005	171,045	2.497	590.321
11 s	18,732	206,052	2.410	574.231
15 s	18,120	271,800	2.435	592.207
19 s	19,349	267,631	2.270	609.24
28 s	19,796	554,288	2.283	602.798

The results from the simulation process using EDEM software described in previous sections showed some differences and similarities among DEM models when a different number of subspheres were used to provide the approximate form of the sesame particle. In addition, although all simulations employed the same material parameters, some differences were found (*e.g.*, the angles of repose and particle density). The discrepancy could be found in an artificial interlocking between particles, caused by the waviness resulting from the use of multi-spherical particles, as the internal friction of the assembly of particles increases caused by the effect of this interlocking. Comparisons between the experimental and simulated results of both external and internal static angles of

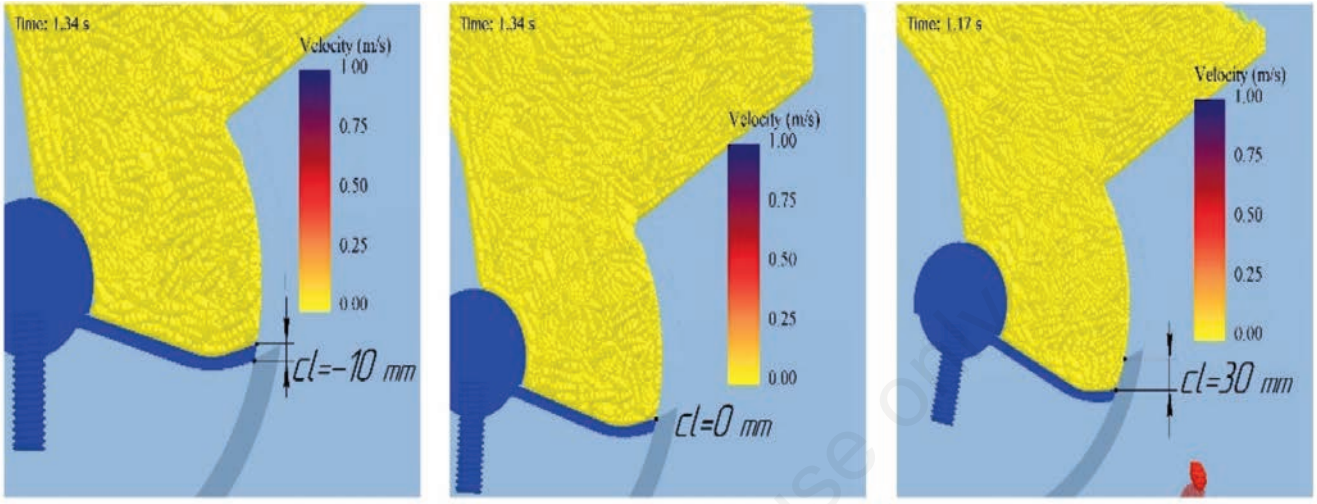

Figure 8. Schematic map of seed exit hole clearance (cl) of the oscillating seed meter during the simulation process.

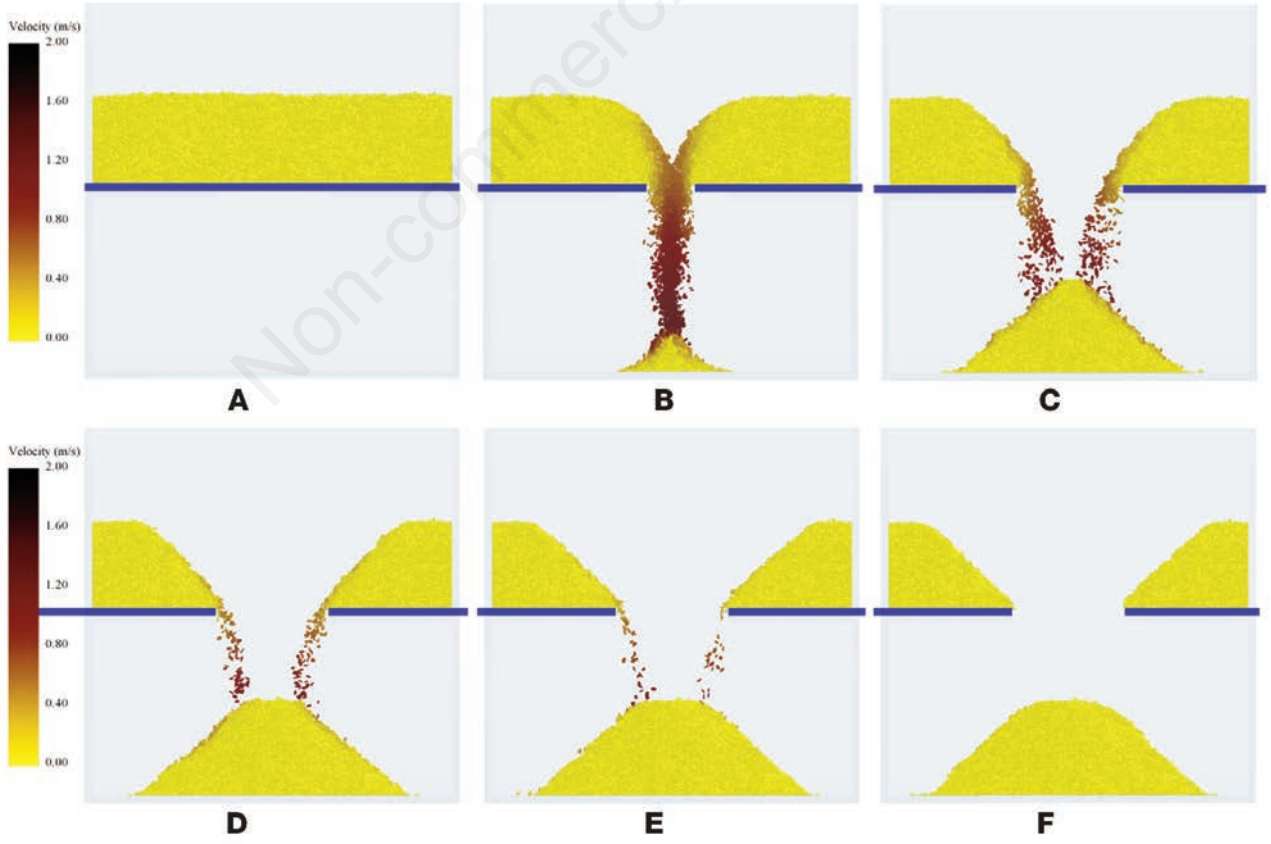

Figure 9. Snapshots showing the piling process simulation of sesame seeds for 28-sphere model, at different discharge times: A) t=0.00 s; B) t=0.50 s; C) t=1.00 s; D) t=1.50 s; E) t=2.00 s; and F) t=3.00 s.

repose for the original sesame and sesame particles are shown in Figure 10. An analysis of results obtained from modelling indicated that the external and internal static angle of repose decreased with the increase in the number of filling spheres for all used sesame models, except for the internal static angle for the 15-sphere model. The mean external angle of repose values for 9, 11, 15, 19, and 28-sphere models are between 46.8° to 51.4°, while the mean internal angle of repose values for the same sesame models are between 43° to 46.7°. In addition, the simulation results showed that the sesame particles models; 15, 19, and 28-sphere gave closer values with the actual sesame seed for the angles of repose and particle density compared with the 9- and 11-sphere models. Briefly, when the number of filling spheres for building sesame particles was 19 or 28, the simulated results were closer to those obtained experimentally, including the static angle of repose (external and internal) and obtained particle density in pilling tests.

As described above, it is concluded on a preliminary basis that the optimal number of filling spheres for irregularly shaped sesame seeds is 19 and 28 sub-spheres, respectively. There were slight differences between them for the internal angle of repose and obtained particle density and about a 1.6° difference in the external static angle of repose (Figure 10).

Comparison and analysis of simulation with the initial experimental results

In this stage, it is essential to consider the hypothesis tests for the statistical equality of the two variances of the compared samples, which allows us to compare the average obtained experimental results for the operation of the oscillating seed metering device with the simulation results. Therefore, there is a need to check the correspondence between the values in the two samples for the general populations to the normal distribution law. The experiments were performed with 20 repetitions, and the number of sesame seeds falling from the exit holes by the oscillating plate for each oscillatory motion was monitored. Thus, the averages of these values were regarded as experimental results for the sesame seed outflow from the oscillating seed meter. Based on the obtained results, we created histograms with six equal sections and put a hypothesis about the normal sample distribution law according to the distribution type of obtained samples (Figure 11). After selecting the Fisher's F-test as an appropriate test for the hypothesis test, the average values of sesame seeds, which are fallen from the oscillating seed meter by the oscillating plate for each oscillatory motion, and the standard size deviation were determined for experimental were $a_{exp.}$=3.831, and $S^2_{exp.}$=0.5486, while for simulated results were $a_{sim.}$=3.722, and $S^2_{sim.}$=0.3834. Comparing the empirical and theoretical frequencies of the two samples using Pearson's chi-squared test were $x^2_{exp.}$=1.4785 and $x^2_{sim.}$=2.1871. According to the table of critical points at a significance level a=0.05 and the number of degrees of freedom k=3, we find x^2_{tab}=7.82 (referred to as x^2_{crit} in the table). While $x^2<x^2_{crit}$; therefore, the hypothesis of normal data distribution for the sample must then be accepted. We calculated t_{Calc} and compared it to tabulated values (t_{tab}) at the degrees of freedom k=38 and the significance level a=0.05 to test the null hypothesis for the statistical equality of the two sample centres. As a result, their values were t_{Calc}=0.7289 and t_{tab}=2.0211 respectively. Since $t_{Calc}<t_{tab}$ the null hypothesis is accepted with a confidence level of 0.95 and the distribution results obtained are statistically equal.

Test results and analysis of the effect of seed exit hole clearance on sesame flow rate

The clearance and the position of the oscillating seed plate could affect the flow rate of the sesame seeds from the oscillating seed metering device. Therefore, clearance with different values was determined, and DEM was used to simulate how the clearance would affect the sesame flow rate. Based on the clearance scheme map shown in Figure 12, computer-based simulation and regression analysis were combined to optimise the parameters of the oscillating seed metering structures. To investigate and analyse the effects of the seed exit hole clearances on the sesame outflow of the oscillating metering device, the EDEM was used for various oscillating seed metering clearances for optimal sesame flow rate performance. Each clearance under different conditions was repeated five times and simulated on the DEM software EDEM.

The simulated and experimental results showed that when the clearance was changed from –10 to +30 mm, the sesame flow rate for each seed exit hole varied from 2.4 to 10 g/min. According to the results for the effect of seed exit hole clearance in the oscillating seed meter on sesame flow rate, the optimum clearance range

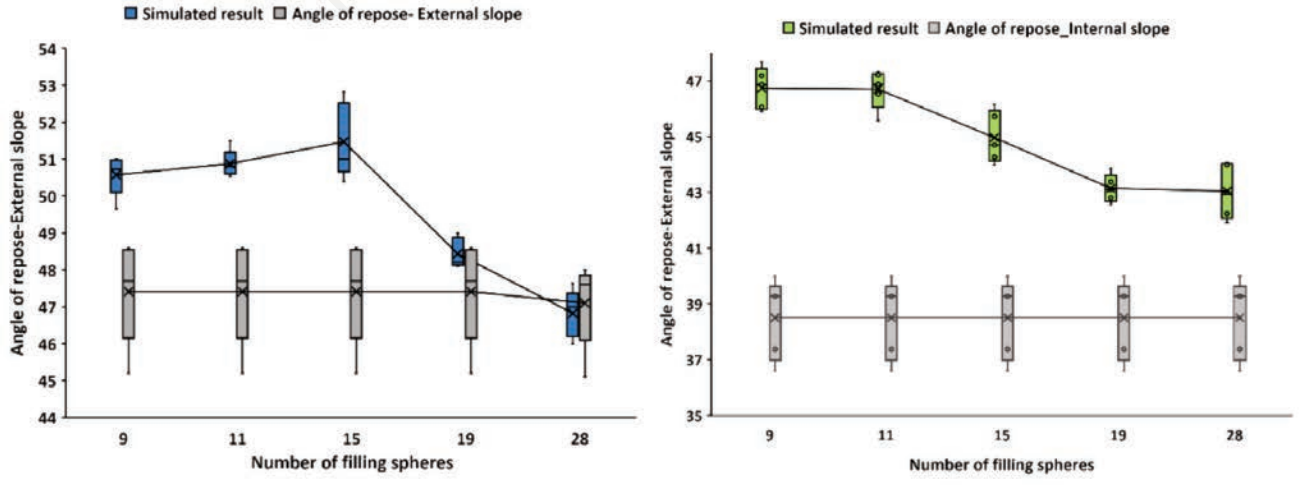

Figure 10. Variations of the external and internal angles of repose for a different number of filling spheres for a sesame seed.

for sowing sesame seeds using the oscillating seed metering device was from 3 to 13 mm, as shown in Figure 12. As a result, this clearance range with a 5 mm interval was used to determine the optimum operating parameters of sesame flow rate from the oscillating seed metering device, as illustrated in Table 3.

Oscillating seed meter simulation analysis

The geometric model was created using CAD and then imported into EDEM, as shown in Figure 13. We began modelling sesame seed particles with nine spheres and gradually increased their number to achieve sufficient accuracy to build a sesame seed model from a few spheres while maximising properties with the material source. The 19-spheres model matched the sesame density and external angle of repose. However, the internal angle of repose was significantly different, leading to a change in the model and increasing the number of spheres to 28 spheres (A similar behaviour of the influence of various DEM shape representation can be seen in the results provided by Soltanbeigi *et al.* 2021), and similarly reported by Xu *et al.* (2018). Sesame particle model with 28-sphere matched with the real one with sufficient accuracy; thus, a further increase in the number of spheres for building a sesame model will not significantly increase its accuracy but will significantly increase the simulation time. If the operation of any mechanism has to be preliminarily analysed using sesame seeds, less accurate models than 9 and 11-sphere can be used. Using these models will reduce the simulation time, but the results will be less accurate. Therefore, such models for different simulated seeds are desirable.

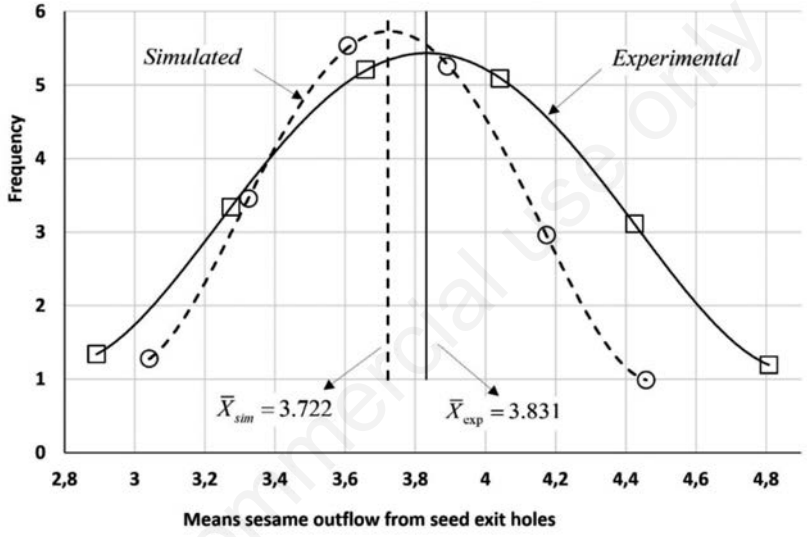

Figure 11. Experimental and simulated outflow distribution for sesame seeds and 28-sphere sesame particle model from the oscillating seed metering device.

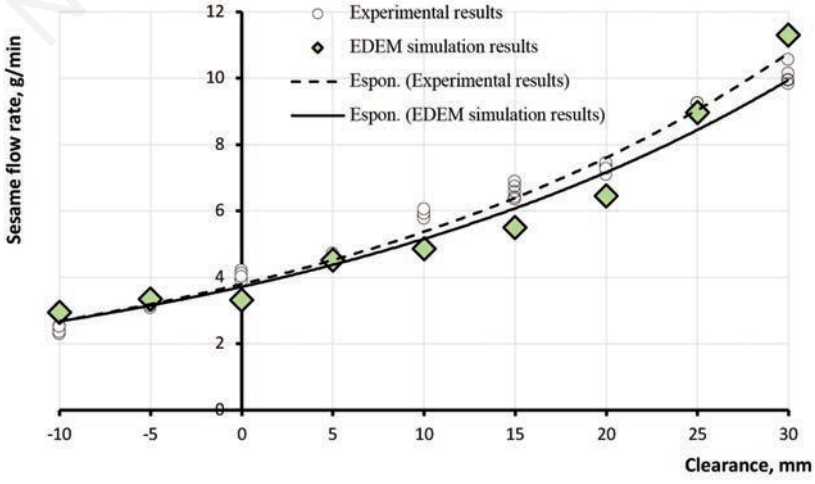

Figure 12. The effects of the seed exit hole clearance on sesame outflow in laboratory and simulation experiments in the oscillating seed metering device.

According to the simulation analysis of the piling test, the simulation results of the 28-sphere model for sesame particles are closer to those obtained experimentally. Therefore, a 28-sphere model was selected as a particle model during the simulation process for the oscillating metering device based on the discrete element approach [which is in agreement with results reported by Markauskas and Kačianauskas (2011); Weigler and Mellmann (2014); Chen *et al.* (2018)]. The simulation conditions were similar to the experimental one to analyse the working process and oscillating seed meter performance (Figure 13). The input parameters for simulations are shown in Table 2. The simulation process was performed to predict the sesame particle flow rate from the oscillating metering device. During the simulation analysis, the outflow process of sesame particles was monitored using a sensor near and opposite the oscillating seed meter exit holes. The sesame particles' outflow was recorded for simulated time (8 s), with a time step is 2.45×10^{-6} s. The number of sesame particles used in the simulation process was 11,947 particles.

The analysis of the obtained data and graphs enabled the optimal parameters values of the oscillating seed metering for sowing sesame seeds, which are as follows: the clearance (*cl*) between the upper edge of the seed exit hole and the upper edge of the oscillating seed plate was 9 mm; opening time *(t)* for oscillating seed plate was 0.022 sec; the angle of motion for the oscillating seed plate (α) was 20º as shown in Figure 14. With these parameters, the seed flow rate was 3.58 g/min, which gives a seeding rate of 2.7 kg/ha for sowing sesame seeds under the working speed of 8 km/hr. with a stable simultaneous ejection of two sesame seeds from the exit hole.

Economic efficiency determination

The modernised version is represented by the *MTZ-82.1* tractor and the vegetable seeder «*Клён-4,2*» with a working width of 4.2 meters and 8 rows for sowing sesame seeds. The seeder is supported by a modernised oscillating seed metering capable of delivering sesame seeds with a flow rate of up to 8 kg/ha while maintaining the average seed flow rate from the seed exit hole with two seeds. The main economic effect is achieved by increasing the operating speed of the seeding machine-tractor up to 8 km/hr. The estimated economic impact is about 2000 $, with a payback period of about seven months. Furthermore, the calculation of economic efficiency has confirmed the rationality of using an oscillating seed meter with a developed control system.

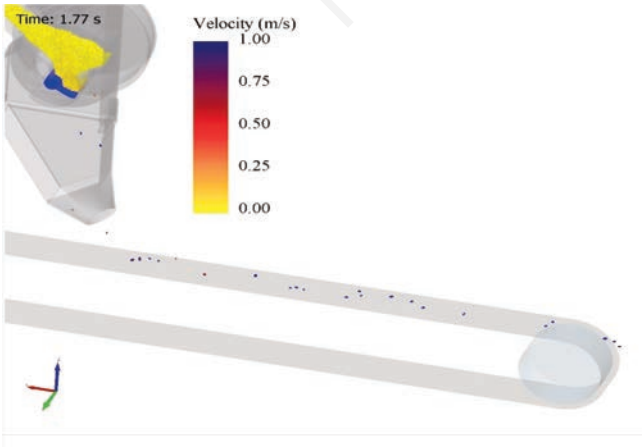

Figure 13. Schematic of oscillating seed metering system in simulation.

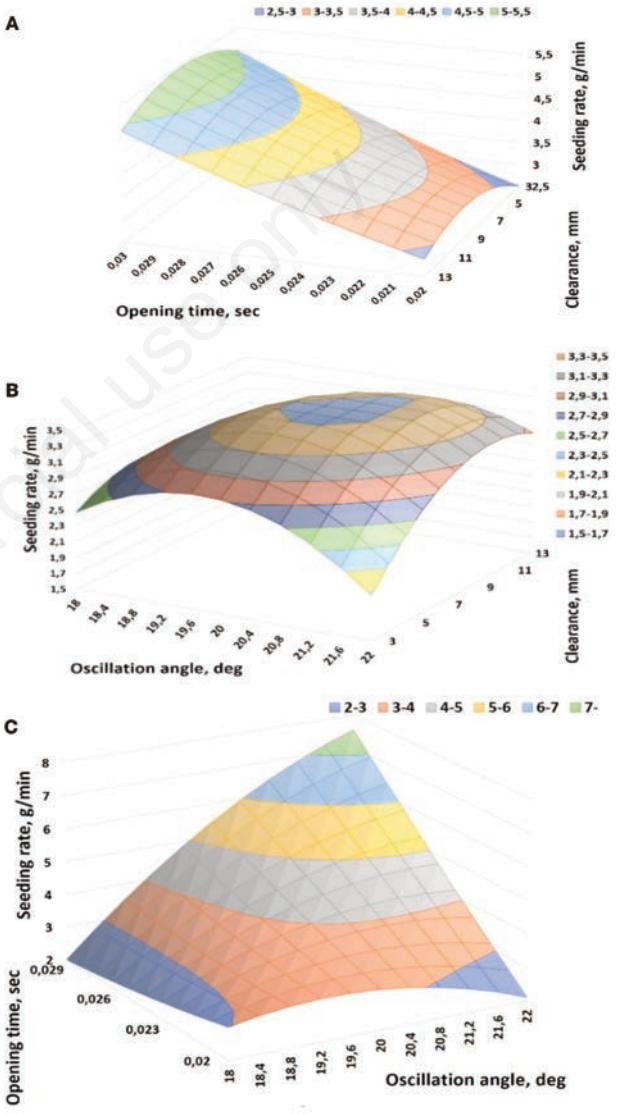

Figure 14. Dependencies of factors: A) the response surface, characterising the change in the opening time t of the oscillating sowing device plate from the clearance cl between the upper point of the cylinder exit hole and the oscillating sowing device plate; B) the response surface, characterising the change in the oscillating angle α of the oscillating sowing device plate from the clearance cl between the upper point of the cylinder exit hole and the oscillating sowing device plate; C) the response surface, characterising the change in the opening time t of the oscillating sowing device plate from the value of the oscillating angle α of the oscillating sowing device plate.

Conclusions

In this work, the sizes of the sesame seeds were measured and analysed. The modelling approach for sesame seeds particle assembly was proposed and verified by comparing the experimental and simulated results in the piling test and oscillating seed metering device. The following conclusions are based on the obtained data from the current study:

i) According to the simulated results in both piling tests and verification of the oscillating metering device, the 28-sphere model for sesame particles was highly consistent with those obtained experimentally. In pilling tests, the simulated results for the static angles of repose (internal and external) and obtained particle density were (43° and 46.8°) and 602.798 kg/m^3, which are closer to the laboratory results (41.1° and 46.8°), and 603 kg/m^3 for static angles of repose (internal and external) and obtained particle density, respectively. Therefore, the results show that the 28-sphere model was appropriate for modelling the sesame seed particle and verifying the feasibility and validity of the modelling method of sesame particles that we suggested in this study. Thus, it is not advisable to further increase the number of spheres.

ii) A solid digital model of the operation of an oscillating sowing device was created. The obtained data from the oscillating seed metering motion parameters, such as the opening time (t), and oscillation angle (α), enabled simulation modelling to be performed and obtain a new theoretical dependence of the influence of the seed exit hole clearance on the sesame seeding rate. The sesame flow rate for each seed tube varied from 2.4 g/min to 10 g/min when the clearance was changed from –10 mm to +30 mm with a fixed oscillation angle (α=20°) and an opening time (t=25 msec). The obtained dependencies allowed us to determine the required seed consumption during the operation of the oscillating seed metering device when the clearance changes and correlate it with agricultural requirements for the seeding rate.

iii) As a result of experimental tests, factors were identified that significantly affect the process of sowing seeds with an oscillating seed device, such as clearance, opening time, and oscillation angle. A control unit for controlling these factors was created using operational parameters set by the microcontroller to control a stepper motor driving the seed metering device.

iv) Processing of the simulated and experimental results allowed us to obtain optimal operational parameters, such as a seed exit hole clearance of 9 mm, which is approximately equal to the average thickness of the sesame seeds used in the experiments. Moreover, we obtained an oscillation angle equal to 20°, and an opening time of 0.022 sec. All these parameters affect the sesame flow rate from the oscillating seed metering device, which was 3.58 g/min, providing a given sesame seed rate of 2.7 kg/ha.

v) Calculation of economic efficiency has confirmed the rationality of using an oscillating seed metering device with a newly developed control system. For example, when sesame is cultivated in a model farm with a sown area of 156 hectares and a payback period of about seven months, the estimated economic effect is $ 2000.

vi) Using the design and parameters of the oscillating seed metering device in the manufacture of precision seeders is a promising development direction.

The EDEM simulation was performed for the sesame seed outflow process using the sesame particle model proposed in this work. It gave a good prediction of the outflow for sesame seeds from the oscillating seed metering device, providing a reference for the design and optimisation of the oscillating seed meter for sesame seed sowing.

References

Boac J.M., Ambrose R.P.K., Casada M.E., Maghirang R.G., Maier D.E. 2014. Applications of discrete element method in modeling of grain postharvest operations. Food Eng. Rev. 6:128-49.

Boac J.M., Casada M.E., Maghirang R.G., Harner J.P. 2010. Material and interaction properties of selected grains and oilseeds for modeling discrete particles. Trans. ASABE 53:1201-16.

Borchani C., Besbes S., Blecker C.H., Attia H. 2010. Chemical characteristics and oxidative stability of sesame seed, sesame paste, and olive oils. J. Agric. Sci. Technol. 12:585-96.

Chen Z., Yu J., Xue D., Wang Y., Zhang Q., Ren L. 2018. An approach to and validation of maize-seed-assembly modelling based on the discrete element method. Powder Technol. 328:167-83.

Cundall P.A., Strack O.D.L. 1979. A discrete numerical model for granular assemblies. Geotechnique 29:47-65.

Guo Y., Wassgren C., Ketterhagen W., Hancock B., Curtis J. 2012. Some computational considerations associated with discrete element modeling of cylindrical particles. Powder Technol. 228:193-8.

Härtl J., Ooi J. Y. 2008. Experiments and simulations of direct shear tests: porosity, contact friction and bulk friction. Granul. Matter 10:263-71.

Hongxin L., Lifeng G., Lulu F., Shifa T. 2015. Study on multi-size seed-metering device for vertical plate soybean precision planter. Int. J. Agric. Biol. Eng. 8:1-8.

Horabik J., Molenda M. 2016. Parameters and contact models for DEM simulations of agricultural granular materials: A review. Biosyst. Eng. 147:206-25.

Jia H., Chen Y., Zhao J., Guo M., Huang D., Zhuang J. 2018. Design and key parameter optimization of an agitated soybean seed metering device with horizontal seed filling. Int. J. Agric. Biol. Eng. 11:76-87.

Johnston L.J., Goihl J., Shurson G.C. 2009. Selected additives did not improve flowability of DDGS in commercial systems. Appl. Eng. Agric. 25:75-82.

Khatchatourian O. A., Binelo M. O., de Lima R. F. 2014. Simulation of soya bean flow in mixed-flow dryers using DEM. Biosyst. Eng. 123:68-76.

Kruggel-Emden H., Rickelt S., Wirtz S., Scherer V. 2008. A study on the validity of the multi-sphere Discrete Element Method. Powder Technol. 188:153–65.

Leblicq T., Smeets B., Ramon H., Saeys W. 2016. A discrete element approach for modelling the compression of crop stems. Comput. Electron. Agric. 123:80-8.

Lei X., Liao Y., Liao Q. 2016. Simulation of seed motion in seed feeding device with DEM-CFD coupling approach for rapeseed and wheat. Comput. Electron. Agric. 131:29-39.

Li Y., Xiantao H., Tao C., Dongxing Z., Song S., Zhang R., Mantao W. 2015. Development of mechatronic driving system for seed meters equipped on conventional precision corn planter. Int. J. Agric. Biol. Eng. 8:1-9.

Lin X., Ng T. 1995. Contact detection algorithms for three-dimensional ellipsoids in discrete element modelling. Int. J. Numer.

Anal. Methods Geomech. 19:653-9.
Markauskas D., Kačianauskas R. 2011. Investigation of rice grain flow by multi-sphere particle model with rolling resistance. Granul. Matter 13:143-8.
Markauskas D., Ramírez-Gómez Á., Kačianauskas R., Zdancevičius E. 2015. Maize grain shape approaches for DEM modelling. Comput. Electron. Agric. 118:247-58.
Noorka I.R., Hafiz S.I., El-Bramawy M.A.S. 2011. Response of sesame to population densities and nitrogen fertilization on newly reclaimed sandy soils. Pak. J. Bot 43:1953-8.
Ouadfel H., Rothenburg L. 1999. An algorithm for detecting inter-ellipsoid contacts. Comput. Geotech. 24:245-63.
Radvilaitė U., Ramírez-Gómez Á., Kačianauskas R. 2016. Determining the shape of agricultural materials using spherical harmonics. Comput. Electron. Agric. 128:160-71.
Ramírez A., Nielsen J., Ayuga F. 2010. On the use of plate-type normal pressure cells in silos: Part 2: Validation for pressure measurements. Comput. Electron. Agric. 71:64-70.
Ren B., Zhong W., Chen Y., Chen X., Jin B., Yuan Z., Lu Y. 2012. CFD-DEM simulation of spouting of corn-shaped particles. Particuology 10:562-72.
Sharaby N., Butovchenko A. 2019. Cultivation technology of sesame seeds and its production in the world and in Egypt. IOP Conf. Ser. Earth Environ. Sci. 403:012093.
Sharaby N., Doroshenko A., Butovchenko A. 2020. Simulation of Sesame Seeds Outflow in Oscillating Seed Metering Device Using DEM. Eng. Technol. Syst. 30:219-31.
Soltanbeigi B., Podlozhnyuk A., Kloss C., Pirker, S. 2021. Influence of various DEM shape representation methods on packing and shearing of granular assemblies. Granul. Matter 23:1-16.
Wang X., Yu J., Lv F., Wang Y., Fu H. 2017. A multi-sphere based modelling method for maize grain assemblies. Adv. Powder Technol. 28:584-95.
Weigler F., Mellmann, J. 2014. Investigation of grain mass flow in a mixed flow dryer. Particuology 12: 33-9.
Xu T., Yu J., Yu Y., Wang Y. 2018. A modelling and verification approach for soybean seed particles using the discrete element method. Adv. Powder Technol. 29:3274-90.
Zhou Y.C., Wright B.D., Yang R.Y., Xu B.H., Yu A.-B. 1999. Rolling friction in the dynamic simulation of sandpile formation. Phys. A Stat. Mech. Its Appl. 269:536-53.